Superlattices and Microstructures 61 (2013) 115–123

Contents lists available at SciVerse ScienceDirect

Superlattices and Microstructures

journal homepage: www.elsevier.com/locate/superlattices

Effect of annealing temperature and CuO on microstructure and optical band gap of $Cu_xZn_{1-x}O$ thin films

Jianguo Lv [a,b,c], Zhitao Zhou [b], Feng Wang [b], Changlong Liu [b], Wanbing Gong [b], Jielin Dai [b,*], Xiaoshuang Chen [a,*], Gang He [c], Shiwei Shi [c], Xueping Song [c], Zhaoqi Sun [c,*], Feng Liu [d]

[a] National Laboratory for Infrared Physics, Shanghai Institute of Technical Physics, Chinese Academy of Sciences, Shanghai 200083, China
[b] School of Electronic and Information Engineering, Hefei Normal University, Hefei 230061, China
[c] School of Physics and Material Science, Anhui University, Hefei 230039, China
[d] School of Mathematics and Physics, Anhui Polytechnic University, 241000 Wuhu, China

ARTICLE INFO

Article history:
Received 2 May 2013
Received in revised form 10 June 2013
Accepted 12 June 2013
Available online 22 June 2013

Keywords:
$Cu_xZn_{1-x}O$
Sol–gel
Thin films
Optical band gap
Photoluminescence

ABSTRACT

$Cu_xZn_{1-x}O$ thin films were prepared by the sol–gel process. Microstructure, surface topography and optical properties were studied by X-ray diffractometry, atom force microscopy, UV–Vis spectrophotometer and fluorescence spectrometer. The monoclinic CuO phase has been observed in $Cu_xZn_{1-x}O$ ($x = 0.05$, 0.10, and 0.15) thin films annealed at 800 °C. Preferential *c*-axis orientation of the $Cu_xZn_{1-x}O$ thin films annealed at 800 °C increases with the increase of *x* value. The annealing temperature and CuO component have great effect on the absorption coefficient of $Cu_xZn_{1-x}O$ thin films in the visible region. The decrease of optical band gap may be attributed to the reduction of the fraction of the amorphous phase and stoichiometry deficiency of ZnO due to CuO doping. The deep level emission in ZnO thin film originates from oxygen vacancy and oxygen interstitial defects. The violet emission peaked at about 400 nm has been assigned to the electron transition from zinc interstitial level and the valence band.

* Corresponding authors. Tel.: +86 551 3674132; fax: +86 551 3674131 (X. Chen).
E-mail addresses: djl@hftc.edu.cn (J. Dai), xschen@mail.sitp.ac.cn (X. Chen), szq@ahu.edu.cn (Z. Sun).

0749-6036/$ - see front matter © 2013 Elsevier Ltd. All rights reserved.
http://dx.doi.org/10.1016/j.spmi.2013.06.010

1. Introduction

Zinc oxide (ZnO), a direct wide band gap (3.37 eV) semiconductor, has stimulated great research interest due to its unique optical and electrical properties that are useful for solar cells [1], gas sensors [2], piezoelectric nanogenerators [3], photocatalyst [4], and so on. As an important photocatalyst, ZnO nanomaterials will play a significant role in environmental protection. The development of photocatalysts under visible light irradiation is one of the challenging tasks in the field of photocatalysis. Hence, for ZnO nanomaterials, redshift in optical band gap and enhancement of visible light absorption have been though as an effective way to utilize solar energy and enhance its photocatalytic activity under visible light. In order to decrease optical band gap and/or enhance visible light absorption, ZnO doped with many dopant such as Cd [5], In [6], Cu [7], Fe [8], Co [9] and so on have been prepared. Annealing temperature also has an important effect on optical band gap of ZnO [10,11]. Recently, the semiconductors nanocomposite thin film has stimulated much research interest due to the coupling of two semiconductors possessing different energy levels. Optical, electrical, photocatalytic and gas sensing properties of CuO combination with other semiconductors such as TiO_2, SnO_2, Cu_2O, WO_3, and ZnO have been widely studied [12–19]. However, the effect of CuO on the optical band gap of ZnO thin film has been seldomly studied [20]. In this letter, $Cu_xZn_{1-x}O$ thin films were prepared on quartz glass by sol–gel method. Effect of annealing temperature and CuO doping on microstructure, surface topography, optical band gap and photoluminescence spectra of the $Cu_xZn_{1-x}O$ thin films were investigated.

2. Experiments details

Zinc acetate dehydrate ($Zn(CH_3COO)_2{\cdot}2H_2O$) and copper nitrate trihydrate ($Cu(NO_3)_2{\cdot}3H_2O$) were dissolved in ethylene glycol monomethyl ether, and then monoethanolamine (MEA) was added to the solution. The concentration of metal ions in $Cu_xZn_{1-x}O$ sols were controlled at 0.5 M and Cu^{2+} was varied from 0 to 0.15 (for x values). The molar ratio of monoethanol amine to zinc acetate was kept at 1:1. The solution was stirred at 60 °C for 2 h to get a homogeneous sol. The quartz glass substrates were cleaned ultrasonically in acetone and deionized water, and dried in hot air. Spin coating was usually made one day after the solution was prepared. $Cu_xZn_{1-x}O$ thin films were deposited on substrate by spin coating with 3000 rpm for 30 s. After coating, the substrates were dried at 150 °C for 10 min. The above process of coating and drying was repeated ten times to obtain the desired thickness. The as-coated thin films were then inserted into a furnace and annealed in air.

Thin film thickness was investigated by surface profiler (Ambios XP-2). The average thickness of the thin films was about 252 nm. The crystal structure of the thin films were examined using a X-ray diffractometry (XRD, MACM18XHF) with Cu Kα radiation ($\lambda = 0.15405$ nm) operating at 40 kV and 100 mA. The 2θ scan range was 30–80° with a step of 0.02° and a scan speed of 8°/min. Surface topography was measured using an atom force microscopy (AFM, CSPM4000) operating in contact mode taken over a scale of 800 × 800 nm. Optical transmittance spectra were measured using a UV–Vis spectrophotometer (UV–Vis, SHIMADZU UV2550) at normal incident of light in the wavelength range of 300–900 nm. The PL spectra were examined in the wavelength range of 350–600 nm at room temperature by fluorescence spectrometer (FL, HITACHI F-4500) with a xenon lamp as light source operating at 325 nm.

3. Results and discussion

Fig. 1 shows XRD patterns of ZnO thin films annealed at temperature of 500, 600, 700 and 800 °C. XRD patterns of $Cu_{0.05}Zn_{0.95}O$, $Cu_{0.1}Zn_{0.9}O$ and $Cu_{0.15}Zn_{0.85}O$ thin films annealed at temperature of 800 °C are shown in Fig. 2. It can be seen from Fig. 1 that nine peaks appear at $2\theta = 31.77°$, 34.42°, 36.26°, 47.53°, 56.60°, 62.86°, 66.37°, 67.95° and 69.09° in the patterns are assigned to (100), (002), (101), (102), (110), (103), (200), (112) and (201) planes of the hexagonal phase ZnO (JCPDS 36-1451). Two peaks appear at $2\theta = 35.50°$ and 38.73° in the Fig. 2 are assigned to (002) and (111) planes of the monoclinic phase CuO (JCPDS 45-0937). The peak positions of the ZnO component in the patterns have no obvious change, but the relatively intensity of diffraction peaks have obvious

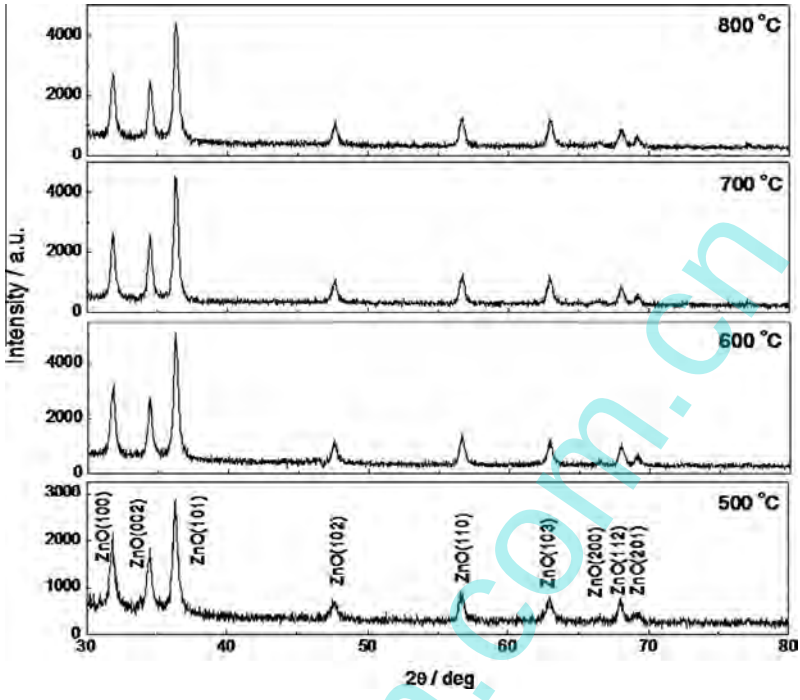

Fig. 1. XRD patterns of ZnO thin films annealed at different temperature.

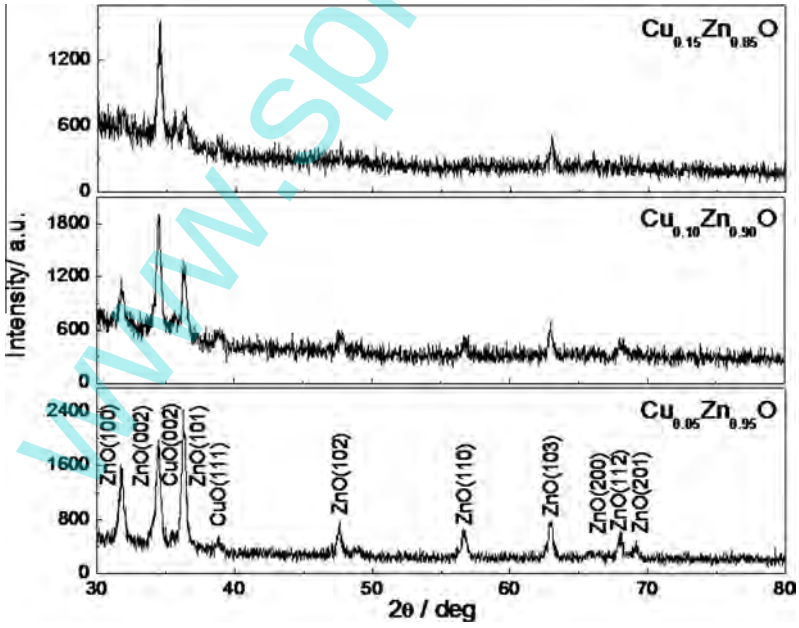

Fig. 2. XRD patterns of $Cu_xZn_{1-x}O$ thin films annealed at temperature of 800 °C.

change. This suggests that the $Cu_xZn_{1-x}O$ (x = 0.05, 0.10, and 0.15) thin films consist of ZnO and CuO phases, and the two oxides combine together primarily through inter-granular coupling instead of intra-granular coupling. Quantitative information concerning the preferential crystallite orientation of hexagonal phase ZnO has been obtained from the texture coefficient $TC_{(hkl)}$ defined as [21]

$$TC_{(hkl)} = \frac{I_{(hkl)}/I_{0(hkl)}}{\frac{1}{N}\sum_N I_{(hkl)}/I_{0(hkl)}} \quad (1)$$

where $I_{(hkl)}$ is the measured relative intensity of the (hkl) plane, $I_{0(hkl)}$ is the standard intensity of the (hkl) plane taken from the JCPDS 36-1451 data, and N is the total number of reflection peaks from the thin film. The value, $TC_{(hkl)} = 1$, represents the thin film with randomly oriented crystallites, while higher value indicates the abundance of crystallites oriented along (hkl) direction. The calculated texture coefficients TC are listed in Table 1. The results reveal that all the TC values of (002) plane of ZnO component are larger than 1, indicating that all the thin films are polycrystalline with preferred orientation along the c-axis perpendicular to substrate surface. For the ZnO thin films, the sample annealed at 700 °C has the largest TC values of (002) plane. The TC value of (002) plane increases with the increase of x value for the $Cu_xZn_{1-x}O$ thin films annealed at 800 °C. Therefore, the crystallinity and preferred orientation along the c-axis of ZnO component can be controlled easily by using annealing temperature and CuO doping.

Fig. 3 show the AFM images of ZnO thin films annealed at temperature of 500, 600 700 and 800 °C. Fig. 4 show the AFM images of $Cu_{0.05}Zn_{0.95}O$, $Cu_{0.1}Zn_{0.9}O$ and $Cu_{0.15}Zn_{0.85}O$ thin films annealed at temperature of 800 °C. Root mean square (RMS) roughness, calculated from AFM images corresponding to $Cu_xZn_{1-x}O$ thin films, is listed in Table 1. It can be seen that average particle size of ZnO thin films increases with the increase of annealing temperature. Many voids between particles have been observed in the ZnO thin films annealed at 600 °C. The ZnO thin film annealed at 800 °C has the largest RMS roughness value. For the thin films annealed at 800 °C, the CuO component makes the decrease of voids between particles. The $Cu_{0.05}Zn_{0.95}O$ thin film, which consists of compact and homogeneous particles, has the smallest RMS roughness value. With x increase from 0 to 0.15, the RMS roughness decreases first and then increases.

Optical transmittance spectra were obtained at room temperature in the range 300–900 nm. The absorption coefficient (α) is calculated from the optical transmittance spectra using the following relation [22]:

$$\alpha = \ln(1/T)/d \quad (2)$$

where T is the optical transmittance and d is the thin film thickness. Fig. 5 illustrates the absorption coefficients of ZnO thin films. Fig. 6 shows the absorption coefficients of $Cu_xZn_{1-x}O$ thin films annealed at 800 °C. It can be seen that all the samples have an abrupt absorption edge in the range of 370–430 nm. For the ZnO thin films, the absorption coefficient increases in the visible region with increasing annealing temperature. The increase of the absorption coefficient in the visible region with increasing the annealing temperature has also been observed by other researchers [23]. The increase of the absorption coefficients of the thin films may be attributed to the increase of defects [8]

Table 1
Optical band gap, RMS roughness and texture coefficient TC of $Cu_xZn_{1-x}O$ thin films.

Sample	Annealing temperature (°C)	Texture coefficient (TC)			RMS roughness (nm)	E_g (eV)
		$TC_{(100)}$	$TC_{(002)}$	$TC_{(101)}$		
ZnO	500	1.17	1.20	0.85	1.13	3.29
ZnO	600	1.157	1.28	0.98	1.59	3.26
ZnO	700	1.03	1.30	0.98	1.49	3.26
ZnO	800	1.93	1.07	0.85	1.76	3.25
$Cu_{0.05}Zn_{0.95}O$	800	0.96	1.54	0.85	1.33	3.24
$Cu_{0.1}Zn_{0.9}O$	800	0.81	1.88	0.58	1.61	3.20
$Cu_{0.15}Zn_{0.85}O$	800	0.75	2.18	0.43	2.05	3.13

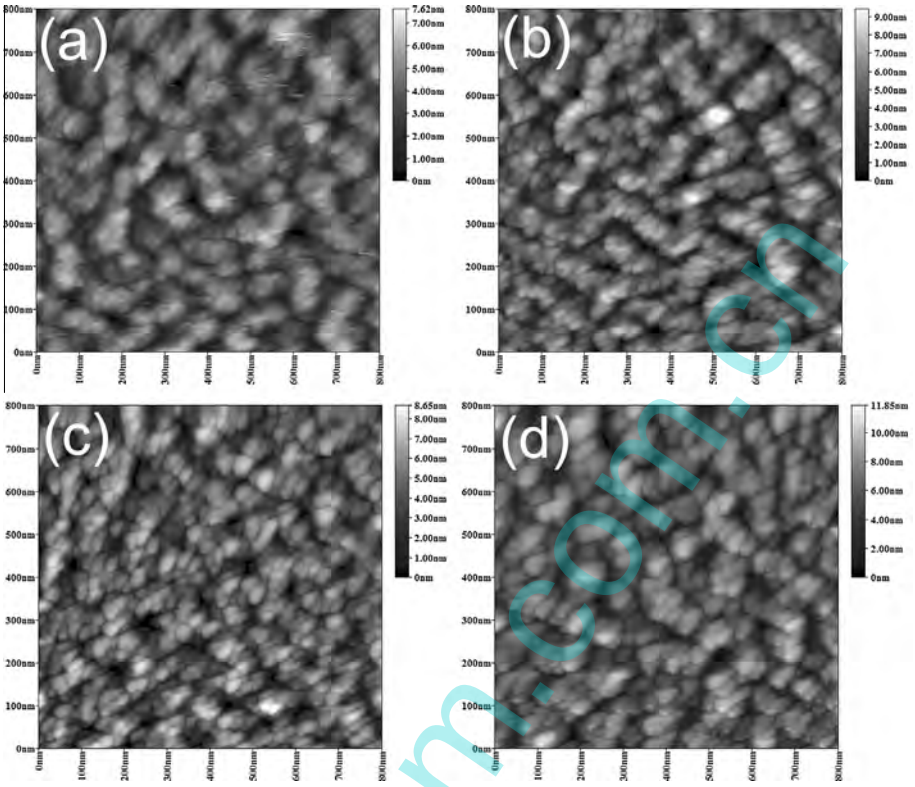

Fig. 3. AFM images of ZnO thin films annealed at temperature of (a) 500 °C, (b) 600 °C, (c) 700 °C and (d) 800 °C.

introduced by higher annealing temperature. Compared with ZnO thin film annealed at 800 °C, the absorption coefficients in the visible region of $Cu_{0.15}Zn_{0.85}O$ thin film annealed at 800 °C obviously increase. The increase of the absorption may be due to the increase of CuO component [24]. It suggests that high CuO component has great effect on the optical absorption of $Cu_xZn_{1-x}O$ thin films.

As a direct band gap semiconductor, the relationship between absorption coefficient (α) of the $Cu_xZn_{1-x}O$ thin films and incident phonon energy ($h\nu$) can be expresses as follow [25]:

$$(\alpha h\nu)^2 = A(h\nu - E_g) \tag{3}$$

where E_g is the optical band gap of the thin films and A is a constant. The $(\alpha h\nu)^2$ versus $h\nu$ plots for $Cu_xZn_{1-x}O$ thin films are shown in Fig. 7. The optical band gap can be calculated by extrapolating the straight linear portion of the plots between $(\alpha h\nu)^2$ and $h\nu$ to the energy axis. The measured optical band gap E_g values are given in Table 1. It can be seen that the E_g decreases from 3.29 to 3.25 eV as annealing temperature increase from 500 to 800 °C. Shan and Yu [26] think that the exponential decay behaviour of E_g values in Al doped ZnO can be attributed to the composition variation in the thin film. Hong et al. [27] attributed the optical band gap red shift of ZnO thin films to the increase of the ZnO grain size. The decrease of optical band gap E_g value is also attributed to the decrease of the fraction of the amorphous ZnO phase in thin films [28]. In our case, as shown from the XRD results, the crystallinity of the ZnO thin film annealed at low temperature is lower than that annealed at high temperature. Therefore, the decrease of optical band gap is due to the reduction of the fraction of the amorphous phase in ZnO thin films. It also can be seen that the E_g decreases from 3.25 to 3.13 eV as x value increases from 0 to 0.15. Zhang and Tang [12] observed the reduction of the optical band gap in the CuO-doped TiO_2 thin films as increasing CuO doping concentration. Sanchez and Lopez

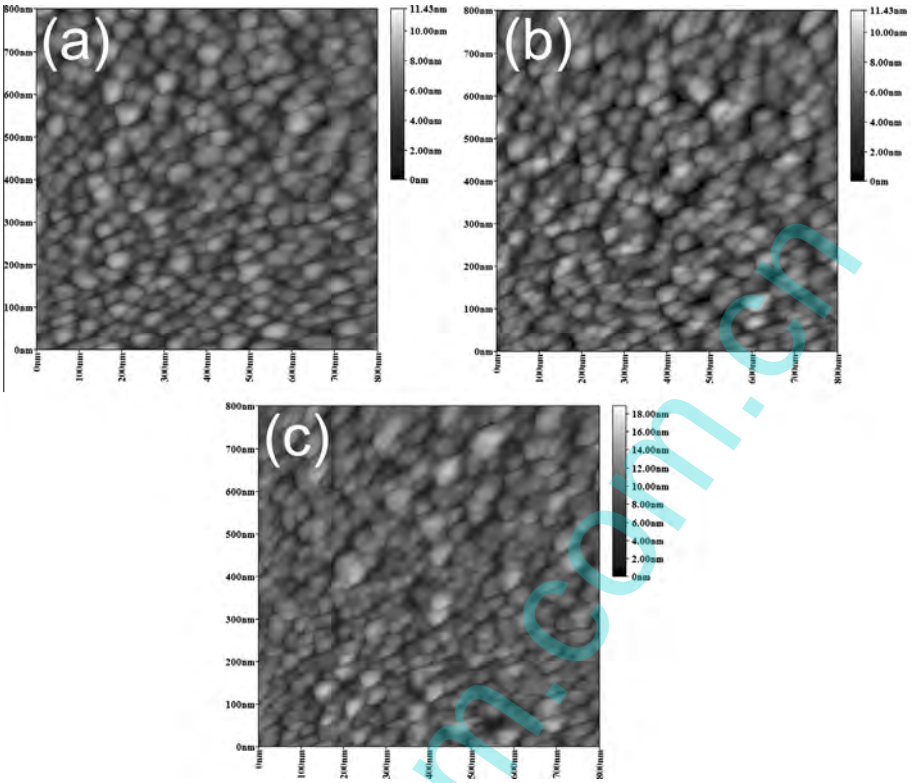

Fig. 4. AFM images of $Cu_{0.05}Zn_{0.95}O$ (a), $Cu_{0.1}Zn_{0.9}O$ (b) and $Cu_{0.15}Zn_{0.85}O$ (c) thin films annealed at temperature of 800 °C.

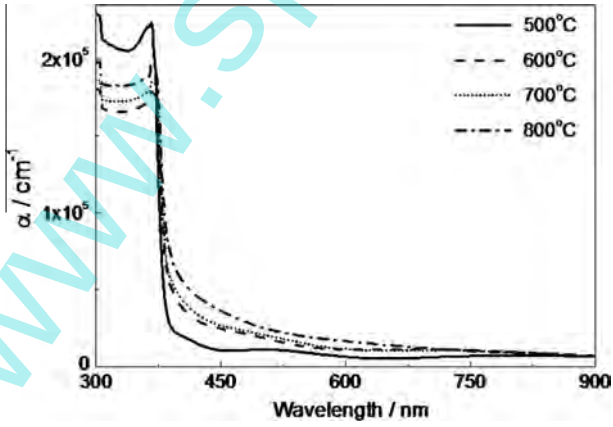

Fig. 5. Absorption coefficients of ZnO thin films annealed at different temperature.

[29] consider that the smaller optical band gap should be attributed to the stoichiometric deficiency of Ti/O ratio. In our case, the reduction of optical band gap of $Cu_xZn_{1-x}O$ thin films may be caused by the stoichiometry deficiency of ZnO due to CuO doping [24]. The considerable improvement of ZnO photocatalytic activity under visible light irradiation is expected to achieve due to the enhanced visible light absorption of the CuO doping.

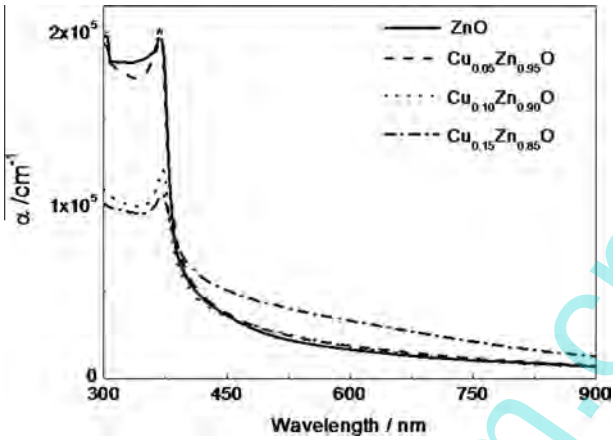

Fig. 6. Absorption coefficients of $Cu_xZn_{1-x}O$ thin films annealed at 800 °C.

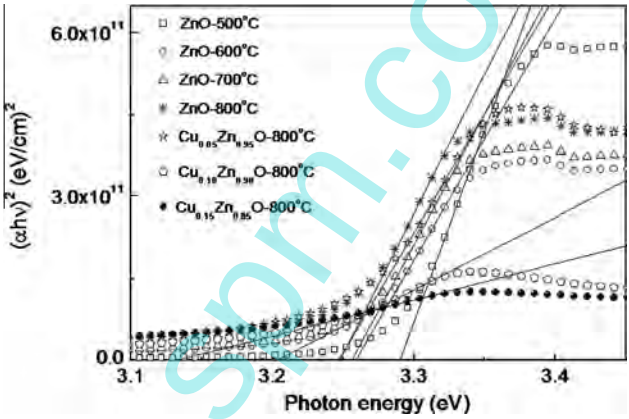

Fig. 7. The $(\alpha h\nu)^2$ versus $h\nu$ plots for $Cu_xZn_{1-x}O$ thin films.

Fig. 8 shows the PL spectra of ZnO thin films annealed at different temperatures. The ZnO thin film annealed at 500 °C shows a violet emission band around 400 nm. The ZnO thin film annealed at 600 °C shows two main peaks composed of a violet emission band centered at 400 nm and a weak deep level emission band centered at 576 nm. As annealing temperature increase from 600 to 800 °C, the intensity of the deep level emission abruptly increases, and the peak of violet emission redshifts from 400 to 405 nm, but that of deep level emission blueshifts from 576 to 538 nm. The violet emission centered at ~400 nm in ZnO may be attributed to the electron–hole recombination between Zinc interstitial (Zn_i) level and the valence band. As can be seen from Fig. 8, the deep level emission of the ZnO thin film annealed at 800 °C consists of orange, yellow and green emission. The origin of the deep level emission has been controversial for decades. It is generally recognized that the orange-red emission in ZnO is due to electron transition from zinc interstitial (Zn_i) to oxygen interstitial (O_i) [30]. The yellow emission in ZnO is due to electron transition from conduction band to oxygen interstitial (O_i) [31]. The green emission in ZnO can be attributed to the electron transition from zinc interstitial (Zn_i) to oxygen vacancy (V_o) defect levels [32]. Therefore, it is believed that the number of oxygen vacancy (V_o) and oxygen interstitial (O_i) defects in ZnO thin film were gradually increased with the increasing of annealing temperature. Fig. 9 shows the PL spectra of $Cu_{0.05}Zn_{0.95}O$, $Cu_{0.10}Zn_{0.90}O$ and $Cu_{0.15}Zn_{0.85}O$ thin films

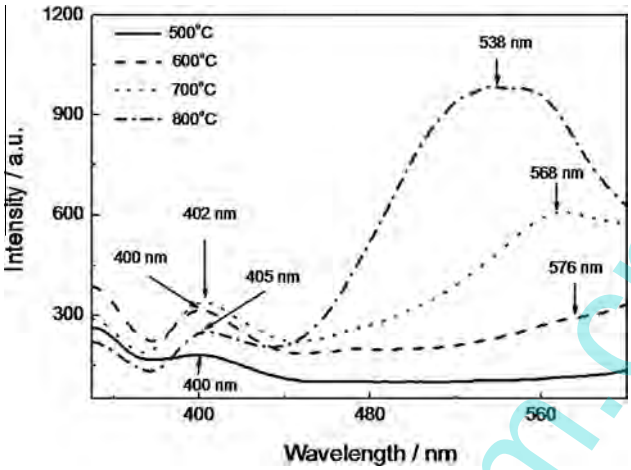

Fig. 8. PL spectra of ZnO thin films annealed at different temperatures.

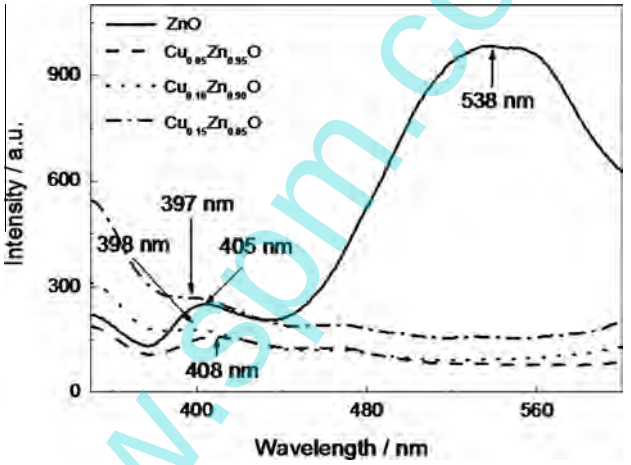

Fig. 9. PL spectra of $Cu_{0.05}Zn_{0.95}O$, $Cu_{0.10}Zn_{0.90}O$ and $Cu_{0.15}Zn_{0.85}O$ thin films annealed at 800 °C.

annealed at 800 °C. It can be seen that with the incorporation of CuO, the deep level emission bands in the PL spectra of the thin films disappear. This may be attributed to the reduction of defects [33], such as oxygen vacancy (V_o) and oxygen interstitial (O_i), which are caused by CuO doping. The peak of violet emission of the thin films annealed at 800 °C redshifts first and then blueshifts with the x value increase from 0 to 0.15.

4. Conclusions

Microstructure, surface topography, optical transmittance spectra and photoluminescence spectra of $Cu_xZn_{1-x}O$ thin films, prepared by the sol–gel method, were measured by XRD, AFM, UV–Vis spectrophotometer and fluorescence spectrometer. The $Cu_xZn_{1-x}O$ (x = 0.05, 0.10, and 0.15) thin films are composed of hexagonal phase ZnO and monoclinic phase CuO. For the $Cu_xZn_{1-x}O$ thin films annealed at 800 °C, with the x value increase from 0 to 0.15, the TC value of (002) plane increases from 1.07 to

2.18, the RMS roughness decreases first and then increases, and the optical band gap E_g decreases from 3.25 to 3.13 eV. The violet emission was assigned to the electron–hole recombination between Zinc interstitial (Zn_i) level and the valence band. The deep level emission in ZnO thin film may be attributed oxygen vacancy and oxygen interstitial defects, which are caused by high annealing temperature.

Acknowledgments

This work was supported by National Natural Science Foundation of China (Nos. 51072001, 51272001, 51002156, 51102072), China Postdoctoral Science Foundation (No. 2012M520944), Anhui Provincial Natural Science Foundation (No. 1208085MF99, 1208085QA16), Shanghai Postdoctoral Science Foundation (No. 12R21416800), Natural Science Foundation of Anhui Higher Education Institution of China (No. KJ2010B148), Funds for Distinguished Young Scholar of Anhui University (No. KJJQ1103).

References

[1] C.-T. Chen, F.-C. Hsu, Y.-M. Sung, H.-C. Liao, W.-C. Yen, W.-F. Su, Y.-F. Chen, Sol. Energy Mater. Sol. Cells 107 (2012) 69–74.
[2] P. Singh, V.N. Singh, K. Jain, T.D. Senguttuvan, Sens. Actuators B: Chem. 166–167 (2012) 678–684.
[3] C.-J. Chang, Y.-H. Lee, C.-A. Dai, C.-C. Hsiao, S.-H. Chen, N.P.D. Nurmalasari, J.-C. Chen, Y.-Y. Cheng, W.-P. Shih, P.-Z. Chang, Microelectron. Eng. 88 (2011) 2236–2241.
[4] Z. Han, L. Ren, Z. Cui, C. Chen, H. Pan, J. Chen, Appl. Catal. B: Environ. 126 (2012) 298–305.
[5] A.D. Acharya, S. Moghe, R. Panda, S.B. Shrivastava, M. Gangrade, T. Shripathi, D.M. Phase, V. Ganesan, Thin Solid Films 525 (2012) 49–55.
[6] M. Caglar, S. Ilican, Y. Caglar, Thin Solid Films 517 (2009) 5023–5028.
[7] C.C. Vidyasagar, Y.A. Naik, T.G. Venkatesh, R. Viswanatha, Powder Technol. 214 (2011) 337–343.
[8] C. Wang, Z. Chen, Y. He, L. Li, D. Zhang, Appl. Surf. Sci. 255 (2009) 6881–6887.
[9] C.-Y. Kao, J.-D. Liao, C.-W. Chang, R.-Y. Wang, Appl. Surf. Sci. 258 (2011) 1813–1818.
[10] R.K. Sendi, S. Mahmud, Appl. Surf. Sci. 261 (2012) 128–136.
[11] S.-S. Lin, J.-L. Huang, P. Šajgalik, Surf. Coat. Technol. 185 (2004) 254–263.
[12] X. Zhang, A. Tang, Mater. Express 2 (2012) 238–244.
[13] S. Xu, A.J. Du, J. Liu, J. Ng, D.D. Sun, Int. J. Hydrogen Energy 36 (2011) 6560–6568.
[14] X.-J. Zheng, Y.-J. Wei, L.-F. Wei, B. Xie, M.-B. Wei, Int. J. Hydrogen Energy 35 (2010) 11709–11718.
[15] S.L. Wang, P.G. Li, H.W. Zhu, W.H. Tang, Powder Technol. 230 (2012) 48–53.
[16] H. Widiyandari, A. Purwanto, R. Balgis, T. Ogi, K. Okuyama, Chem. Eng. J. 180 (2012) 323–329.
[17] N. Datta, N. Ramgir, M. Kaur, S. Kailasa Ganapathi, A.K. Debnath, D.K. Aswal, S.K. Gupta, Sens. Actuators B: Chem. 166–167 (2012) 394–401.
[18] L. He, H. Cheng, G. Liang, Y. Yu, F. Zhao, Appl. Catal. A: Gen. 452 (2013) 88–93.
[19] R. Saravanan, S. Karthikeyan, V.K. Gupta, G. Sekaran, V. Narayanan, A. Stephen, Mater. Sci. Eng. C 33 (2013) 91–98.
[20] A. Zainelabdin, S. Zaman, G. Amin, O. Nur, M. Willander, Appl. Phys. A 108 (2012) 921–928.
[21] S. Lemlikchi, S. Abdelli-Messaci, S. Lafane, T. Kerdja, A. Guittoum, M. Saad, Appl. Surf. Sci. 256 (2010) 5650–5655.
[22] J. Lü, J. Dai, J. Zhu, X. Song, Z. Sun, J. Wuhan Univ. Technol.-Mater. Sci. Edit. 26 (2011) 23–27.
[23] S.W. Xue, X.T. Zu, W.L. Zhou, H.X. Deng, X. Xiang, L. Zhang, H. Deng, J. Alloys Compd. 448 (2008) 21–26.
[24] P. Sathishkumar, R. Sweena, J.J. Wu, S. Anandan, Chem. Eng. J. 171 (2011) 136–140.
[25] A. Sarkar, S. Ghosh, S. Chaudhuri, A.K. Pal, Thin Solid Films 204 (1991) 255–264.
[26] F.K. Shan, Y.S. Yu, Thin Solid Films 435 (2003) 174–178.
[27] R. Hong, J. Huang, H. He, Z. Fan, J. Shao, Appl. Surf. Sci. 242 (2005) 346–352.
[28] F.K. Shan, G.X. Liu, W.J. Lee, B.C. Shin, J. Appl. Phys. 101 (2007) 053106–053108.
[29] E. Sanchez, T. Lopez, Mater. Lett. 25 (1995) 271–275.
[30] X.L. Wu, G.G. Siu, C.L. Fu, H.C. Ong, Appl. Phys. Lett. 78 (2001) 2285–2287.
[31] M. Liu, A.H. Kitai, P. Mascher, J. Lumin. 54 (1992) 35–42.
[32] C.H. Ahn, Y.Y. Kim, D.C. Kim, S.K. Mohanta, H.K. Cho, J. Appl. Phys. 105 (2009) 013502–013505.
[33] J.X. Wang, X.W. Sun, Y. Yang, K.K.A. Kyaw, X.Y. Huang, J.Z. Yin, J. Wei, H.V. Demir, Nanotechnology 22 (2011) 325704.